J. theor. Biol. (2002) **216,** 501–512
doi:10.1006/yjtbi.3000, available online at http://www.idealibrary.com on IDEAL®

Intercellular Coupling Mechanism for Synchronized and Noise-Resistant Circadian Oscillators

HIROKI R. UEDA*†‡, KENZO HIROSE† AND MASAMITSU IINO†

†*Department of Pharmacology, Graduate School of Medicine, The University of Tokyo, Bunkyo-ku, Tokyo* 113, *Japan and* ‡*Molecular Medicine Research Laboratories, Institute for Drug Discovery Research, Yamanouchi Pharmaceutical Co., Ltd.*, 21 *Miyukigaoka, Tsukuba-shi, Ibaraki* 305-8585, *Japan*

(*Received on* 13 *June* 2001, *Accepted in revised form on* 22 *February* 2002)

The circadian clock in multicellular organisms consists of multiple autonomous single-cell oscillators. These individual oscillator cells produce coherent oscillations even in the presence of internal noise associated with rhythm-generating reaction rates and in the absence of external time cues such as light and temperature. Thus, an intercellular coupling mechanism must synchronize the cells to induce coherent circadian oscillations. We propose the roles of a synchronizing factor that is secreted from individual cells during subjective day to induce light-pulse-type phase shifts in the neighboring cells or, alternatively, a factor that is secreted during subjective night to induce dark-pulse-type phase shifts. Here, we present our multicellular stochastic model of *Drosophila* circadian rhythms that emulates the intercellular coupling mechanism and suggest that the mechanism facilitates the constancy of the circadian rhythm with possible functional redundancy among different synchronizing factors.

Introduction

The *Drosophila* circadian clock is one of the best characterized circadian systems (Dunlap, 1999; Pittendrigh, 1993; Williams & Sehgal, 2001). In *Drosophila*, like many other organisms, several genes are involved in sustaining the circadian rhythm, namely *period* (*per*) (Konopka & Benzer, 1971), *timeless* (*tim*) (Sehgal *et al.*, 1994), *Drosophila Clock* (*dClk*) (Allada *et al.*, 1998), *Cycle* (*Cyc*) (Rutila *et al.*, 1998) and *double-time* (*dbt*) (Price *et al.*, 1998) (Fig. 1A). Among them, three genes are rhythmically expressed: *per* (Hardin *et al.*, 1990), *tim* (Sehgal *et al.*, 1995) and *dClk* (Bae *et al.*, 1998). *per* and *tim* mRNAs peak early in the evening, whereas *dClk* mRNA peaks at night to early in the morning. Analyses of *per* and *tim* oscillatory expression have revealed a negative *per–tim* feedback loop, in which *per* and *tim* expressions are repressed by PERIOD (PER) and TIMELESS (TIM) heterodimers (PER–TIM) (Darlington *et al.*, 1998). On the other hand, analyses of *dClk* periodic expression have uncovered another inhibitory *dClk* feedback loop, in which *dClk* expression is repressed by two helix-loop-helix-PAS transcription factors, *Drosophila* CLOCK (dCLK) and CYCLE (CYC) (Bae *et al.*, 1998; Darlington *et al.*, 1998; Glossop

*Corresponding author. Department of Pharmacology, Graduate School of Medicine, The University of Tokyo, Bunkyo-ku, Tokyo 113, Japan. Tel.: +81-3-5841-3414; fax: +81-3-5841-3390.
E-mail address: hiro@m.u-tokyo.ac.jp (H.R. Ueda).

0022-5193/02/ $35.00/0

et al., 1999). The *per–tim* feedback loop and *dClk* feedback loop are interlocked with each other because the *per–tim* feedback loop is activated by dCLK and CYC heterodimers (dCLK–CYC) and the *dClk* feedback loop is derepressed by PER–TIM (Glossop *et al.*, 1999). A single cellular deterministic model based on this structure (Fig. 1A) has been shown to be sufficient to reproduce wild-type and several mutant phenotypes (Ueda *et al.*, 2001).

The circadian clock in multicellular organisms consists of multiple autonomous single-cell oscillators (Plautz *et al.*, 1997; Welsh *et al.*, 1995). Importantly, these individual cells produce coherent oscillations (Yamazaki *et al.*, 2000) even in the presence of internal noise, which results from the stochastic nature of reaction events when there are few molecules in a cell (Barkai & Leibler, 2000; McAdams & Arkin, 1999) and in the absence of external time cues such as light and temperature. Moreover, Takahashi's group reported a detailed rhythm analysis on chimeric *Clock*/WT mutant mice that strongly support the importance of intercellular connections of neuronal clock cells (Low-Zeddies & Takahashi, 2001). In order to address how multiple cells produce coherent rhythms in the presence of internal noise without referring to external time cues, we extended the single cellular deterministic model on *Drosophila* circadian rhythms (Ueda *et al.*, 2001) to a three-dimensional 100-cellular stochastic model. We hypothesized the existence of a synchronizing factor that is regulated by the circadian clock, secreted from

FIG. 1. Molecular mechanisms of *Drosophila* circadian rhythms. (A) Interlocked feedback mechanism of *Drosophila* circadian rhythms. *per–tim* feedback loop: Transcription of *per* and *tim* is activated by dCLK–CYC transcriptional activators. PER is destabilized by DBT-dependent phosphorylation. PER and TIM dimerize with each other. PER–TIM heterodimers enter the nucleus. Nuclear PER–TIM heterodimers repress transcription of *per* and *tim* by forming complexes with dCLK–CYC heterodimers. *dClk* feedback loop: *dClk* expression is activated by PER–TIM heterodimers and repressed by dCLK–CYC heterodimers. *per–tim* and *dClk* feedback loops are interlocked with each other to produce anti-phase oscillations of *per* (*tim*) and *dClk* mRNA. (B) Time courses of *per* and *tim* expression simulated with the interlocked feedback model. *per* and *tim* mRNA (blue), PER and TIM monomers (light blue), cytoplasmic (green) and nuclear (light green) PER–TIM heterodimers peak at circadian time (CT) 15.0, 17.3, 17.9 and 21.6, respectively. CT = 0 and CT = 12 are usually defined as dawn and dusk, respectively. In the simulations, we defined CT = 0 as bottom of *per* mRNA expression. Expression patterns of *per* and *tim* mRNA (blue) or PER and TIM monomer (green) are overlapped because identical parameter values are used for *per* and *tim* expression. (C) Time courses of *dClk* expression. *dClk* mRNA (red), dCLK (pink), cytoplasmic (orange) and nuclear (yellow) dCLK–CYC heterodimers peak at CT = 4.0, 7.5, 8.2 and 13.4, respectively.

FIG. 2. Multicellular stochastic models of *Drosophila* circadian rhythms. (A) Simulated time course of *per* mRNA level in the single cellular deterministic model. (B–D) Simulated time course of *per* mRNA level in the 100-cellular stochastic model. Amplitude of average *per* mRNA oscillations is reduced to less than 5% of the amplitude in the deterministic model (B) due to loss of coherence. Despite the identical initial conditions (C), the introduction of 10% noise completely abolishes coherent *per* mRNA oscillations eventually (D). Different colors represent different cells.

FIG. 3. Synchronization mechanisms for coherent oscillations. (A) Magnitude of phase shifts induced by 18 possible synchronizing factors found in "day" systems, in which the synchronizing factors are secreted during subjective day under repression by cytoplasmic PER proteins (inset). (B) Magnitude of phase shifts induced by 20 possible synchronizing factors found in "night" systems, in which the synchronizing factors are secreted during subjective night under activation by nuclear dCLK–CYC heterodimers (inset). (C) Secretion patterns of seven synchronizing factors found in "light-pulse" systems, in which a synchronizing factor induces light-pulse-type phase shifts (inset). (D) Secretion patterns of 10 synchronizing factors found in "dark-pulse" systems, in which a synchronizing factor induces dark-pulse-type phase shifts (inset). Lines with an asterisk represent two overlapping lines. (E) Average *per* mRNA oscillation in a synchronized system. In this system, the secretion of the factor is activated by cytoplasmic PER proteins and the secreted factor promotes degradation of nuclear PER–TIM heterodimers in the neighboring cells. Even from totally different initial conditions, the presence of a synchronization factor restores large and reproducible amplitude of average *per* mRNA oscillation. The time courses of *per* mRNA level in individual cells show coherent oscillations (inset). (F) Average *per* mRNA oscillations in an unsynchronized system. In this system, the secretion of the factor is activated by cytoplasmic PER proteins and the secreted factor represses degradation of nuclear PER–TIM heterodimers in the neighboring cells. *per* mRNA levels in individual cells show totally incoherent oscillations (inset).

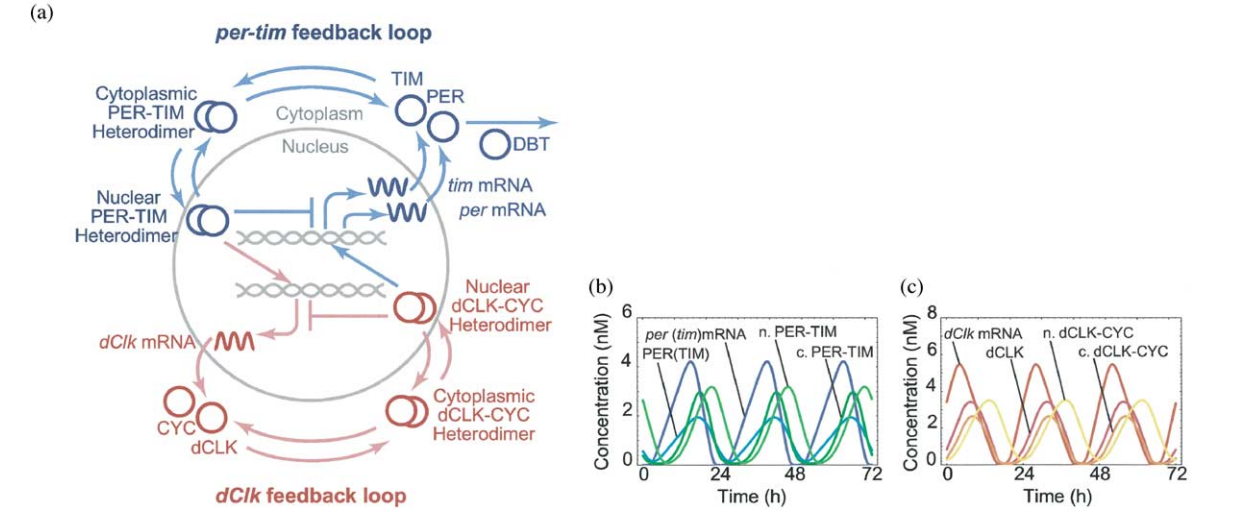
(a)
per-tim feedback loop
Cytoplasmic PER-TIM Heterodimer
Cytoplasm
Nucleus
TIM
PER
DBT
tim mRNA
per mRNA
Nuclear PER-TIM Heterodimer
Nuclear dCLK-CYC Heterodimer
dClk mRNA
CYC
dCLK
Cytoplasmic dCLK-CYC Heterodimer
dClk feedback loop
(b)
per (tim)mRNA
PER(TIM)
n. PER-TIM
c. PER-TIM
Concentration (nM)
Time (h)
(c)
dClk mRNA
dCLK
n. dCLK-CYC
c. dCLK-CYC
Concentration (nM)
Time (h)

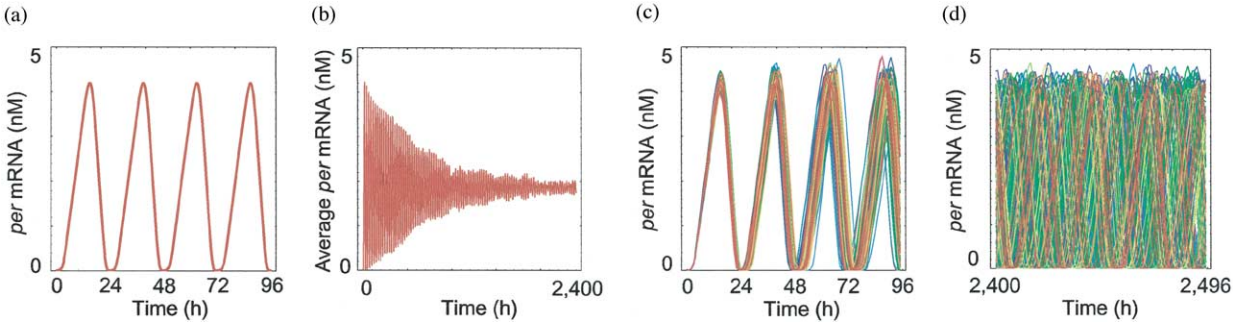
(a)
per mRNA (nM)
Time (h)
(b)
Average per mRNA (nM)
Time (h)
(c)
per mRNA (nM)
Time (h)
(d)
per mRNA (nM)
Time (h)

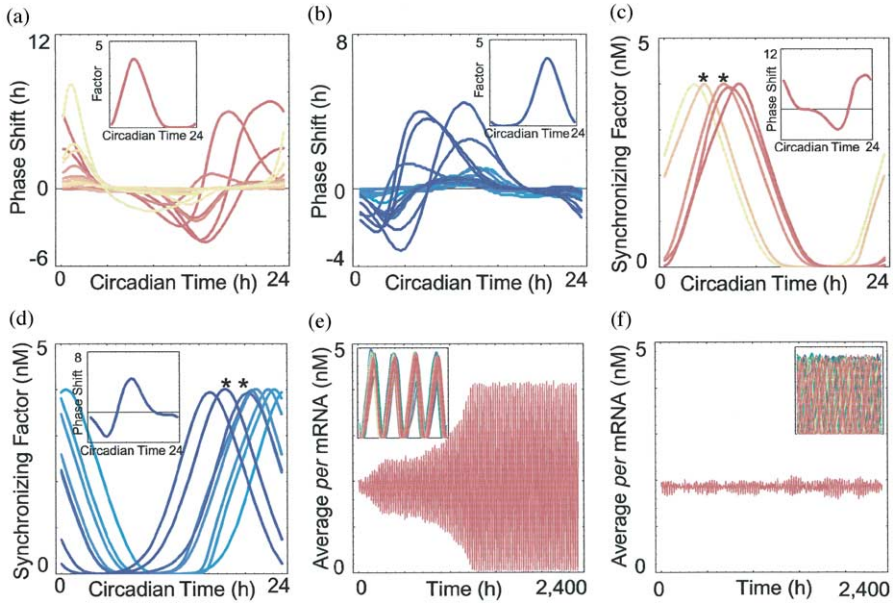
(a)
Phase Shift (h)
Factor
Circadian Time 24
Circadian Time (h)
(b)
Phase Shift (h)
Factor
Circadian Time 24
Circadian Time (h)
(c)
Synchronizing Factor (nM)
Phase Shift
Circadian Time 24
Circadian Time (h)
(d)
Synchronizing Factor (nM)
Phase Shift
Circadian Time 24
Circadian Time (h)
(e)
Average per mRNA (nM)
Time (h)
(f)
Average per mRNA (nM)
Time (h)

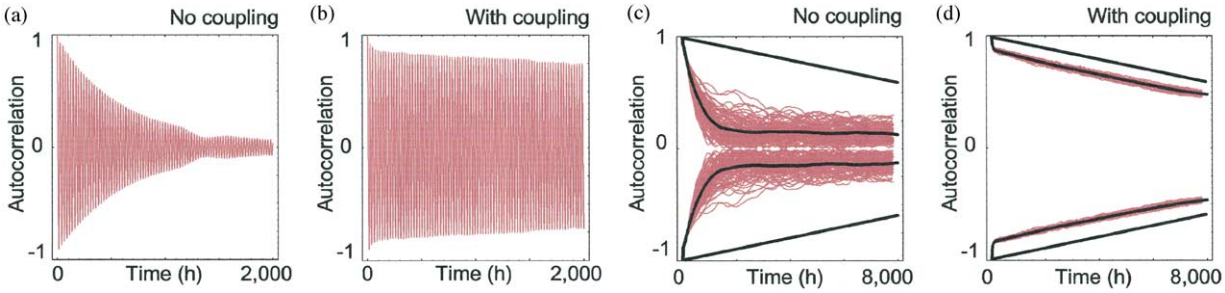

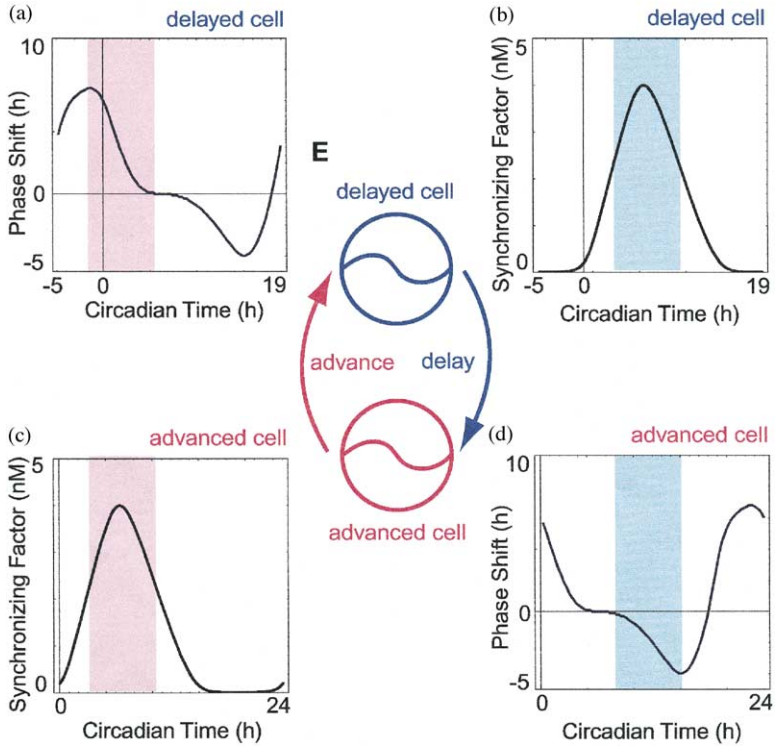

doi: 10.1006 jtbi2002.3000

the cells, and received by the neighboring cells to affect the rate of one of the reactions in the circadian system. Through extensive simulation and analysis, we determined the roles of a synchronizing factor that is secreted from individual cells during subjective day to induce light-pulse-type phase shifts in the neighboring cells or, alternatively, a factor that is secreted during subjective night to induce dark-pulse-type phase shifts. We also found that the intercellular coupling mechanism facilitates noise resistance of the circadian system with possible functional redundancy among different synchronizing factors.

Results

STOCHASTIC SIMULATION OF MULTIPLE CIRCADIAN OSCILLATORS

The rates of reactions in the circadian clock are affected by stochastic noise because limited copy numbers of molecules are involved in the reaction steps within individual cells (Barkai & Leibler, 2000; McAdams & Arkin, 1999). Such inherent noise is expected to perturb the synchrony among clock cells. To assess the effect of noise on the circadian clock, we extended the single-cellular deterministic model of *Drosophila* circadian rhythms to a 100-cellular stochastic model. The *per* mRNA level of the single-cellular deterministic model shows oscillation with a constant period and a large amplitude (Fig. 2A). The multicellular stochastic model shows a dramatically different behavior from the single-cellular deterministic model. Despite the identical initial conditions (Fig. 2C), the introduction of 10% noise to each reaction rate (see Appendix A) completely abolishes coherence in *per* mRNA oscillations in different cells (Fig. 2D) and the averaged amplitude is reduced to less than 5% of that of the deterministic model (Fig. 2B). In reality, multiple clock cells (Plautz *et al.*, 1997; Welsh *et al.*, 1995) exhibit synchronized rhythm even in the absence of external time cues such as light and temperature (Brandes *et al.*, 1996; Yamazaki *et al.*, 2000). Therefore, our model predicts that circadian systems in multicellular organisms require intrinsic mechanisms for synchronization. The basic idea of synchronizing clocks was previously proposed as the "clock-shop" model by Winfree (1975). However, a detailed molecular mechanism of synchronization has not yet been described.

SEARCH FOR SYNCHRONIZATION FACTORS

To elucidate the molecular mechanism of synchronization, we hypothesized the existence of a synchronizing factor that is: (1) located downstream of one of the components of the circadian clock (e.g. activated by dCLK–CYC transcription factors), (2) secreted from the cells and transported through diffusion, and (3) received by the neighboring cells to affect

FIG. 4. Noise tolerance induced by a synchronizing factor. Temporal autocorrelation function of *per* mRNA oscillations in the system with (B) or without (A) a synchronizing factor. The system without synchronization (A) loses autocorrelation rapidly and exponentially whereas the system with synchronization (B) loses autocorrelation slowly and linearly. Envelopes (peaks and bottoms connected, respectively) of the autocorrelation functions of the system with (D) or without (C) synchronization in individual cells (red lines) and data averaged over 100 cells (black line). The system without synchronization maintains half-correlation only for 490 hr on average with large variance whereas the system with synchronization holds half-correlation for 7400 hr on average with small variance. Due to the finite duration of the model (20 000 hr), the envelope of the autocorrelation function of a perfect system declines linearly (dotted lines).

FIG. 5. Schematic explanation of the synchronization mechanism. For simplification, two circadian oscillators having a 5-hour difference in phase are considered (A). Light-pulse-type phase shifts of the delayed (A) and advanced (D) cells, and photic secretion of a synchronizing factor from the delayed (B) and advanced (C) cells are plotted against the subjective circadian time. The advanced cell secretes the factor during subjective day (C), which advances the delayed cell during subjective late night to early day (A). On the other hand, the delayed cell secretes the factor during subjective day (B), which delays the advanced cell during subjective late day to early night (D). These processes reduce the phase difference between cells.

the rate of one of the reactions in the circadian system (e.g. affecting the rate of TIM degradation).

First, in order to determine the appropriate target reaction controlled by the synchronizing factors, we fixed the secretion time course of the potential synchronizing factor and scanned the reaction steps that are controlled by the factor (see Appendix B). We performed two types of simulations: a "day" system, in which a factor is secreted during subjective day under repression by PER (Fig. 3A inset), and a "night" system, in which a factor is secreted during subjective night under activation by nuclear dCLK–CYC (Fig. 3B inset). For each system, we generated 96 variant models, in which the factor either up- or down-regulates one of the 48 reactions in the circadian clock. We found that some of the variant models restored coherent *per* mRNA oscillations (Fig. 3E), whereas others failed to do so (Fig. 3F). As a result, we found 18 and 20 possible target reactions regulated by a synchronizing factor in the day and night systems, respectively. In the "day" system, 18 possible reactions controlled by the synchronizing factor result either in a decrease of nuclear PER–TIM heterodimers or in an increase of nuclear dCLK–CYC heterodimers. On the other hand, 20 possible reactions regulated by the factor in the "night" system lead to an increase of nuclear PER–TIM heterodimers or in a decrease of nuclear dCLK–CYC heterodimers (Table 1).

To elucidate the common characteristics of the found target reaction steps, we analysed alteration of the phase, period and amplitude of *per* mRNA oscillation induced by the synchronization factor. The period and the amplitude of *per* mRNA oscillations are slightly changed (periods range from 22.1 to 25.5 hr, and amplitudes range from 108.8 to 95.5% of that without synchronizing factors). However, no common features of the effects on the period and the amplitude were observed. On the other hand, the phase shifts induced by the regulation of the target reaction

TABLE 1

Reactions regulated by synchronizing factors secreted during subjective day or night

"Day" system*	"Night" system†
PER translation (S_2, i)	PER degradation (D_2, i)
TIM translation (S_4, i)	TIM degradation (D_4, i)
Cytoplasmic PER–TIM degradation (D_5, p)	Cytoplasmic PER–TIM degradation (D_5, i)
Nuclear PER–TIM degradation (D_6, p)	Cytoplasmic PER–TIM unbinding from degradation enzymes (L_5, p)
PER–TIM nuclear import (T_1, i)	Nuclear PER–TIM degradation (D_6, i)
PER–TIM unbinding from nuclear importer (K_1, p)	Nuclear PER–TIM unbinding from degradation enzymes (L_6, p)
PER–TIM nuclear export (T_2, p)	PER–TIM association (V_1, p)
PER–TIM unbinding from nuclear exporter (K_2, i)	PER–TIM dissociation (V_2, i)
PER–TIM unbinding from the *dClk* promoter (A_3, p)	PER–TIM nuclear export (T_2, i)
dCLK–CYC unbinding from the *dClk* promoter (R_3, i)	PER–TIM unbinding from nuclear exporter (K_2, p)
dCLK–CYC association (V_3, p)	dCLK translation (S_6, i)
dCLK–CYC disassociation (V_4, i)	dCLK degradation (D_8, p)
dCLK–CYC nuclear import (T_3, p)	dCLK–CYC association (V_3, i)
dCLK–CYC nuclear export (T_4, i)	dCLK–CYC dissociation (V_4, p)
dCLK–CYC unbinding from nuclear importer (K_3, i)	Cytoplasmic dCLK–CYC degradation (D_9, p)
dCLK degradation (D_8, i)	Nuclear dCLK–CYC degradation (D_{10}, p)
Cytoplasmic dCLK–CYC degradation (D_9, i)	dCLK–CYC nuclear import (T_3, i)
Nuclear dCLK–CYC degradation (D_{10}, i)	Cytoplasmic dCLK–CYC unbinding from nuclear importer (K_3, p)
	dCLK–CYC nuclear export (T_4, p)
	Nuclear dCLK–CYC binding to nuclear exporter (K_4, i)

*In the "day" system, a synchronizing factor is secreted during subjective day under repression by PER proteins.

†In the "night" system, a synchronizing factor is secreted during subjective night under activation by nuclear dCLK–CYC heterodimers. The parameter regulated by the synchronizing factor is indicated in parentheses (for meaning of parameter, see Appendix A). (i) and (p) in parentheses represent inhibition and promotion, respectively, of the reaction by the synchronizing factor.

steps by the synchronizing factor showed an interesting feature. We calculated the phase shift by changing the rate of each target reaction for 1 hr at different circadian time points and measuring the shift of the subsequent peak of *per* mRNA oscillations as compared with that without perturbation (see Appendix C). The magnitude of the phase shift is plotted against the circadian time point at which the reaction rate was controlled (Fig. 3). In 18 cases of the day system, the phase shifts show transition from delay to advance during subjective night, and transition from advance to delay during subjective day (Fig. 3A). On the other hand, 20 phase shifts in the night system show inverse patterns, i.e., transition from delay to advance during subjective day and transition from advance to delay during subjective night (Fig. 3B). Interestingly, these phase shifts in the day and night systems resemble those induced by the light pulse and the dark pulse, respectively (Takahashi *et al.*, 1989).

In the above analyses, we fixed the secretion time course of the potential synchronizing factor and scanned the reaction steps that are affected by the factor. Next, in order to elucidate the appropriate upstream regulation of the synchronizing factor, we also carried out a converse analysis, i.e., we fixed the reaction step that is affected and altered the time course of the secretion of the synchronizing factor. We first chose the factor that induces light-pulse-type phase shifts by promoting nuclear PER–TIM degradation (Fig. 3C inset). We then scanned the time course of the factor such that one of the 10 components of the circadian clock either up- or down-regulates its secretion. Seven samples among 20 possible variant models restored coherent *per* mRNA oscillations (Fig. 3E), whereas others failed to do so (Fig. 3F). In another set of analyses, we chose the factor that induces dark-pulse-type phase shifts by promoting nuclear dCLK–CYC degradation (Fig. 3D inset). When we scanned the time course of the factor, we found 10 possible synchronizing factors in the dark-pulse system (Table 2). All the synchronizing factors in the light-pulse system peak during subjective day (Fig. 3C) while those in the dark-pulse system peak during subjective night or dawn (Fig. 3D). Based on these results, we propose that a factor that satisfies the following characteristics can synchronize the clock cells: a factor that is secreted from individual cells during subjective day to induce light-pulse-type phase shifts in the neighboring cells. Factors with their secretion and phase shift patterns shifted along the circadian time by the same magnitude may also synchronize the clock cells, an example of which is a factor that is secreted during subjective night to induce dark-pulse-type phase shifts.

TABLE 2

Regulators of synchronizing factors inducing light-pulse- or dark-pulse-type phase shifts

"Light-pulse" system*	"Dark-pulse" system†
Nuclear dCLK–CYC (r, 3.3)	Nuclear dCLK–CYC (a, 16.2)
per mRNA (r, 4.4)	*per* mRNA (a, 17.9)
tim mRNA (r, 4.4)	*tim* mRNA (a, 17.9)
PER protein (r, 6.5)	PER protein (a, 20.3)
TIM protein (r, 6.5)	TIM protein (a, 20.3)
dClk mRNA (a, 7.1)	*dClk* mRNA (r, 20.7)
cytoplasmic PER–TIM (r, 8.2)	Cytoplasmic PER–TIM (a, 21.2)
	dCLK protein (r, 22.5)
	Cytoplasmic dCLK–CYC (r, 23.2)
	Nuclear PER–TIM (a, 0.54)

*In the "light-pulse" system, a synchronizing factor induces light-pulse-type phase shifts by promoting PER degradation.

†In the "dark-pulse" system, a synchronizing factor induces dark-pulse-type phase shifts by promoting nuclear dCLK–CYC degradation. (a) and (r) represent an activator and repressor, respectively, on the secretion of the synchronizing factor. Numerical values in the parentheses indicate peak secretion time of the synchronizing factor.

FUNCTIONAL REDUNDANCY AMONG DIFFERENT SYNCHRONIZING FACTORS

The intercellular coupling mechanism proposed here predicts that there are several potential factors that produce coherent oscillations. We examined whether one synchronizing factor would conflict with another. Coherent oscillations are produced in a system having two synchronizing factors, one secreted during subjective day under repression by PER and inducing light-pulse-type phase shifts by promoting nuclear PER–TIM degradation, and the

other secreted during subjective night under activation by nuclear dCLK–CYC heterodimers and inducing dark-pulse-type phase shifts by promoting nuclear dCLK–CYC degradation (data not shown). These two synchronizing factors are functionally redundant because only one of the factors can synchronize oscillators (Fig. 3A and B, Table 1).

NOISE RESISTANCE BY THE SYNCHRONIZING MECHANISM

Internal noise effects on the reaction rates of the circadian clock may also perturb the constancy of the circadian rhythm, although an ability to function reliably in the presence of internal noise is required for the circadian system (Barkai & Leibler, 2000). We examined whether the synchronizing mechanism presented here would satisfy this constraint. We calculated the autocorrelation functions of time series data in the 100-cellular system with or without intercellular coupling (Fig. 4). The system without intercellular coupling loses correlation rapidly (Fig. 4A), whereas the system with intercellular coupling retains correlation for a much longer time (Fig. 4B). The system with intercellular coupling maintains correlation for about 7400 hr (Fig. 4D), which is about 15 times longer than that of the system without intercellular coupling (Fig. 4C). Therefore, owing to a synchronizing factor, the neighboring cells correct each other's deviation to stay in the proper rhythm even in the presence of internal noise. Thus, the intercellular coupling mechanism is important not only for synchronization among multiple clock cells but also for constancy of the circadian rhythm.

Discussion

INTUITIVE EXPLANATIONS FOR THE SYNCHRONIZING MECHANISM

The scheme depicted in Fig. 5 provides a simplified explanation to help us understand how the intercellular coupling mechanism synchronizes multiple circadian oscillators. Let us consider two cells having different phases, one with an advanced phase and the other with a delayed phase, so that there is a 5-hr time difference. The advanced cell secretes a synchronizing factor during subjective day (Fig. 5C). The secreted factor is received by the delayed cell during subjective late night to early day because of the phase difference and advances its phase (Fig. 5A). The delayed cell also secretes the synchronizing factor during subjective day (Fig. 5B). The advanced cell receives the secreted factor during late day to early night because of the phase difference and its phase is delayed (Fig. 5D). Thus, the advanced cell advances the delayed cell while the delayed cell delays the advanced cell (Fig. 5E). These processes reduce the phase difference between cells. The same explanation holds for a synchronizing factor secreted during subjective night if the time axis is shifted by 12 hr. To verify that the intercellular coupling mechanism proposed here is model-independent, we implemented a 100-cellular stochastic model based on Leloup & Goldbeter's (1998) model and obtained similar results (data not shown).

SYNCHRONIZATION IN UNICELLULAR ORGANISMS

Unicellular organisms have cell division cycle periods that are shorter than 24 hr. Cell division cycle greatly affects global changes in transcription and translation rates. Unicellular organisms such as cyanobacteria show clear circadian rhythms in transcription even though the cells divide for less than 24 hr (Kondo *et al.*, 1997; Mori *et al.*, 1996). The intercellular coupling mechanisms proposed here provide a solution to reduce noise and to maintain constant circadian periodicity despite global changes in the state of the cell. Actually, the work done by Hastings' group provided suggestive evidence for synchronization in the unicellular organism *Gonyaulax polyedra* (Broda *et al.*, 1986). They also extracted a substance of low molecular weight, gonyauline, from *Gonyaulax polyedra* and showed that gonyauline shortens the circadian clock period (Roenneberg *et al.*, 1991). Although it is not known whether gonyauline is secreted from the cell, when it is secreted or what type of phase shift it induces, it is interesting to examine the possibility that gonyauline is a synchronization factor.

HETEROGENEOUS ORGANIZATION AND COORDINATION OF CIRCADIAN SYSTEM

In multicellular organisms, cell-type dependent circadian characteristics are known. In *Drosophila*, a limited number of lateral neuron cells direct a long-term-sustaining locomotion activity, while in other peripheral tissues different molecular mechanisms have been suggested (Krishnan *et al.*, 2001). In mammals, cultured suprachiasmatic nucleus (SCN) cells showed a robust circadian rhythm that persisted for up to 32 days *in vitro* (Yamazaki *et al.*, 2000), while liver, lung and skeletal muscle expressed circadian rhythms, which became damped after two or seven cycles *in vitro*. Evidence for the heterogeneous organization of the circadian system raises at least two questions. Is there a difference in molecular mechanism between the peripheral damped oscillators and the central pace-making oscillator? How are these heterogeneous oscillators organized and coordinated to construct circadian systems? Although the detailed molecular mechanisms have not been fully elucidated, it is important to raise these issues, which are important subjects for future studies.

CANDIDATES FOR SYNCHRONIZING FACTORS

What do we know about the candidate substances for the synchronizing factors? In *Drosophila*, it is known that the *pdf* gene product, a humoral peptide hormone (PDF), accumulates in a circadian manner during subjective day in lateral neurons and is positively regulated by the *dClk* gene product (Blau & Young, 1999; Park *et al.*, 2000). Ectopic expression of PDF alters circadian activity rhythms without abolishing the circadian *per*/*tim* expression levels (Helfrich-Forster *et al.*, 2000). Although the phase-shift effects caused by PDF on circadian rhythms in *Drosophila* are unknown, it is important to examine the possibility that PDF may be the synchronization factor. If PDF is a synchronization factor, the phase shift induced by PDF should resemble the light-pulse-type pattern.

In vertebrates, several agonists, including glutamate, GABA, melatonin, serotonin and dopamine, have been reported to be involved in phase shifts induced by external time cues, such as light pulses, and can directly induce phase shifts in circadian clocks (Adachi *et al.*, 1998; Liu & Reppert, 2000; McArthur *et al.*, 1991; Prosser *et al.*, 1990; Shibata *et al.*, 1994). Furthermore, these agonists are secreted periodically in phase with the circadian period even in the absence of external time cues (Adachi *et al.*, 1998; Aguilar-Roblero *et al.*, 1993; Dudley *et al.*, 1998; Hamada *et al.*, 1999; Ikeda *et al.*, 1997; Shinohara *et al.*, 1998). Interestingly, dopamine and melatonin in the pigeon eye show secretion patterns and phase shifts that are quite similar to the ''day-type'' and ''night-type'' synchronizing factors presented here: dopamine peaks in subjective day and induces light-pulse-type phase shifts, whereas melatonin peaks in subjective night and induces dark-pulse-type phase shifts (Adachi *et al.*, 1998). However, the physiological roles of these agonists remain elusive. Our results suggest possible roles into these agonists in synchronization and noise resistance of multiple circadian oscillators and encourage further investigation of the roles of these agents. One caution drawn from the present work is that, due to the possible presence of redundant factors, the blockage or elimination of one putative synchronizing factor may not result in the abolition of synchrony.

We thank H. Iwasaki, T. Kondo, M. Hasegawa, A. Adachi, G. A. Oda, B. Ermentrout for useful information, H. Kitano, M. Hagiwara, S. Onami for critical advice, K. M. Kyoda, M. Morohashi, S. Hamahashi for technical advice, S. Hashimoto, T. Takasugi, T. Horiguchi, S. Iwase for useful discussion, A. Kimura for comment on the manuscript. This work was performed as part of the research and development project of Industrial Science and Technology Program supported by NEDO.

REFERENCES

Adachi, A., Nogi, T. & Ebihara, S. (1998). Phase-relationship and mutual effects between circadian rhythms of ocular melatonin and dopamine in the pigeon. *Brain Res.* **792,** 361–369.

Aguilar-Roblero, R., Verduzco-Carbajal, L., Rodriguez, C., Mendez-Franco, J., Moran, J. & de la Mora, M. P. (1993). Circadian rhythmicity in the GABAergic system in the suprachiasmatic nuclei of the rat. *Neurosci. Lett.* **157,** 199–202.

Allada, R., White, N. E., So, W. V., Hall, J. C. & Rosbash, M. (1998). A mutant *Drosophila* homolog of

mammalian clock disrupts circadian rhythms and transcription of period and timeless. *Cell* **93,** 791–804.

Bae, K., Lee, C., Sidote, D., Chuang, K. Y. & Edery, I. (1998). Circadian regulation of a *Drosophila* homolog of the mammalian Clock gene: PER and TIM function as positive regulators. *Mol. Cell Biol.* **18,** 6142–6151.

Barkai, N. & Leibler, S. (2000). Circadian clocks limited by noise. *Nature* **403,** 267–268.

Blau, J. & Young, M. W. (1999). Cycling vrille expression is required for a functional *Drosophila* clock. *Cell* **99,** 661–671.

Brandes, C., Plautz, J. D., Stanewsky, R., Jamison, C. F., Straume, M., Wood, K. V., Kay, S. A. & Hall, J. C. (1996). Novel features of Drosophila period transcription revealed by real-time luciferase reporting. *Neuron* **16,** 687–692.

Broda, H., Brugge, D., Homma, K. & Hastings, J. W. (1986). Circadian communication between unicells? Effects on period by cell-conditioning of medium. *Cell Biophys.* **8,** 47–67.

Darlington, T. K., Wager-Smith, K., Ceriani, M. F., Staknis, D., Gekakis, N., Steeves, T. D. L., Weitz, C. J., Takahashi, J. S. & Kay, S. A. (1998). Closing the circadian loop: CLOCK-induced transcription of its own inhibitors per and tim. *Science* **280,** 1599–1603.

Dudley, T. E., DiNardo, L. A. & Glass, J. D. (1998). Endogenous regulation of serotonin release in the hamster suprachiasmatic nucleus. *J, Neurosci.* **18,** 5045–5052.

Dunlap, J. C. (1999). Molecular bases for circadian clocks. *Cell* **96,** 271–290.

Gillespie, D. T. (1977). Exact stochastic simulation of coupled chemical reactions. *J. Phys. Chem.* **81,** 2340–2361.

Glossop, N. R., Lyons, L. C. & Hardin, P. E. (1999). Interlocked feedback loops within the *Drosophila* circadian oscillator. *Science* **286,** 766–768.

Hamada, T., Ootomi, M., Horikawa, K., Niki, T., Wakamatu, H. & Ishida, N. (1999). The expression of the melatonin synthesis enzyme: arylalkylamine N-acetyltransferase in the suprachiasmatic nucleus of rat brain. *Biochem. Biophys. Res. Commun.* **258,** 772–777.

Hardin, P. E., Hall, J. C. & Rosbash, M. (1990). Feedback of the *Drosophila* period gene product on circadian cycling of its messenger RNA levels. *Nature* **343,** 536 –540.

Helfrich-Forster, C., Tauber, M., Park, J. H., Muhlig-Versen, M., Schneuwly, S. & Hofbauer, A. (2000). Ectopic expression of the neuropeptide pigment-dispersing factor alters behavioral rhythms in *Drosophila* melanogaster. *J. Neurosci.* **20,** 3339–3353.

Ikeda, M., Azuma, S. & Inoue, S. (1997). Vitamin B12 enhances GABA content but reduces glutamate content in the rat suprachiasmatic nucleus. *Am. J. Physiol.* **273,** R359–R363.

Kondo, T., Mori, T., Lebedeva, N. V., Aoki, S., Ishiura, M. & Golden, S. S. (1997). Circadian rhythms in rapidly dividing cyanobacteria. *Science* **275,** 224–227.

Konopka, R. J. & Benzer, S. (1971). Clock mutants of *Drosophila* melanogaster. *Proc. Natl Acad. Sci. U.S.A.* **68,** 2112–2116.

Krishnan, B., Levine, J. D., Lynch, M. K., Dowse, H. B., Funes, P., Hall, J. C., Hardin, P. E. & Dryer, S. E. (2001). A new role for cryptochrome in a *Drosophila* circadian oscillator. *Nature* **411,** 313–317.

Leloup, J. C. & Goldbeter, A. (1998). A model for circadian rhythms in *Drosophila* incorporating the formation of a complex between the PER and TIM proteins. *J. Biol. Rhythms.* **13,** 70–87.

Liu, C. & Reppert, S. M. (2000). GABA synchronizes clock cells within the suprachiasmatic circadian clock. *Neuron* **25,** 123–128.

Low-Zeddies, S. S. & Takahashi, J. S. (2001). Chimera analysis of the clock mutation in mice shows that complex cellular integration determines circadian behavior. *Cell* **105,** 25–42.

McAdams, H. H. & Arkin, A. (1999). It's a noisy business! Genetic regulation at the nanomolar scale. *Trends Genet.* **15,** 65–69.

McArthur, A. J., Gillette, M. U. & Prosser, R. A. (1991). Melatonin directly resets the rat suprachiasmatic circadian clock *in vitro*. *Brain Res.* **565,** 158–161.

Mori, T., Binder, B. & Johnson, C. H. (1996). Circadian gating of cell division in cyanobacteria growing with average doubling times of less than 24 hours. *Proc. Natl Acad. Sci. U.S.A.* **93,** 10 183–10 188.

Park, J. H., Helfrich-Forster, C., Lee, G., Liu, L., Rosbash, M. & Hall, J. C. (2000). Differential regulation of circadian pacemaker output by separate clock genes in *Drosophila*. *Proc. Natl Acad. Sci. U.S.A.* **97,** 3608–3613.

Pittendrigh, C. S. (1993). Temporal organization: reflections of a Darwinian clock-watcher. *Annu. Rev. Physiol.* **55,** 16–54.

Plautz, J. D., Kaneko, M., Hall, J. C. & Kay, S. A. (1997). Independent photoreceptive circadian clocks throughout *Drosophila*. *Science* **278,** 1632–1635.

Price, J. L., Blau, J., Rothenfluh, A., Abodeely, M., Kloss, B. & Young, M. W. (1998). *double-time* is a novel *Drosophila* clock gene that regulates PERIOD protein accumulation. *Cell* **94,** 83–95.

Prosser, R. A., Miller, J. D. & Heller, H. C. (1990). A serotonin agonist phase-shifts the circadian clock in the suprachiasmatic nuclei *in vitro*. *Brain Res.* **534,** 336–339.

Roenneberg, T., Nakamura, H., Cranmer 3rd, L. D., Ryan, K., Kishi, Y. & Hastings, J. W. (1991). Gonyauline: a novel endogenous substance shortening the period of the circadian clock of a unicellular alga. *Experientia* **47,** 103–106.

Rutila, J. E., Suri, V., Le, M., So, W. V., Rosbash, M. & Hall, J. C. (1998). CYCLE is a second bHLH-PAS clock protein essential for circadian rhythmicity and transcription of *Drosophila* period and timeless. *Cell* **93,** 805–814.

Sehgal, A., Price, J. L., Man, B. & Young, M. W. (1994). Loss of circadian behavioral rhythms and per RNA oscillations in the *Drosophila* mutant timeless. *Science* **263,** 1603–1606.

Sehgal, A., Rothenfluh-Hilfiker, A., Hunter-Ensor, M., Chen, Y., Myers, M. P. & Young, M. W. (1995). Rhythmic expression of timeless: a basis for promoting circadian cycles in period gene autoregulation. *Science* **270,** 808–810.

Shibata, S., Watanabe, A., Hamada, T., Ono, M. & Watanabe, S. (1994). N-methyl-D-aspartate induces

phase shifts in circadian rhythm of neuronal activity of rat SCN *in vitro*. *Am J Physiol* **267,** R360–R364.

Shinohara, K., Honma, S., Katsuno, Y., Abe, H. & Honma, K. (1998). Circadian release of amino acids in the suprachiasmatic nucleus *in vitro*. *Neuroreport* **9,** 137–140.

Takahashi, J. S., Murakami, N., Nikaido, S. S., Pratt, B. L. & Robertson, L. M. (1989). The avian pineal, a vertebrate model system of the circadian oscillator: cellular regulation of circadian rhythms by light, second messengers, and macromolecular synthesis. *Recent. Prog. Horm. Res.* **45,** 279–348.

Ueda, H. R., Hagiwara, M. & Kitano, H. (2001). Robust oscillations within the interlocked feedback model of *Drosophila* circadian rhythm. *J. theor. Biol.* **210,** 401–406.

Welsh, D. K., Logothetis, D. E., Meister, M. & Reppert, S. M. (1995). Individual neurons dissociated from rat suprachiasmatic nucleus express independently phased circadian firing rhythms. *Neuron* **14,** 697–706.

Williams, J. A. & Sehgal, A. (2001). Molecular components of the circadian system in *Drosophila*. *Annu. Rev. Physiol.* **63,** 729–755.

Winfree, A. T. (1975). Unclocklike behaviour of biological clocks. *Nature* **253,** 315–319.

Yamazaki, S., Numano, R., Abe, M., Hida, A., Takahashi, R., Ueda, M., Block, G. D., Sakaki, Y., Menaker, M. & Tei, H. (2000). Resetting central and peripheral circadian oscillators in transgenic rats. *Science* **288,** 682–685.

Appendix A

Stochastic Simulation of Multiple Circadian Oscillators

We previously constructed the following differential equations (see below, Ueda *et al.*, 2001) with 48 system parameters and 10 variables representing concentrations of *per*, *tim* and *dClk* mRNAs (Per^i_m, Tim^i_m and Clk^i_m, i indicates the index of cells), and their respective protein products PER, TIM and dCLK (Per^i_c, Tim^i_c and Clk^i_c); both cytoplasmic and nuclear PER–TIM heterodimers (PT^i_c and PT^i_n) as well as both cytoplasmic and nuclear dCLK–CYC heterodimers (CC^i_c and CC^i_n).

$$\frac{dPer^i_m}{dt} = S_1 \frac{(CC^i_n/A_1)^a + B_1}{1 + (PT^i_n/R_1)^r + (CC^i_n/A_1)^a + B_1} - D_1 \frac{Per^i_m}{L_1 + Per^i_m} - D_0 Per^i_m, \tag{A.1}$$

$$\frac{dPer^i_c}{dt} = S_2 Per^i_m - V_1 Per^i_c Tim^i_c + V_2 PT^i_c - D_2 \frac{Per^i_c}{L_2 + Per^i_c} - D_0 Per^i_c, \tag{A.2}$$

$$\frac{dTim^i_m}{dt} = S_3 \frac{(CC^i_n/A_2)^a + B_2}{1 + (PT^i_n/R_2)^r + (CC^i_n/A_2)^a + B_2} - D_3 \frac{Tim^i_m}{L_3 + Tim^i_m} - D_0 Tim^i_m, \tag{A.3}$$

$$\frac{dTim^i_c}{dt} = S_4 Tim^i_m - V_1 Per^i_c Tim^i_c + V_2 PT^i_c - D_4 \frac{Tim^i_c}{L_4 + Tim^i_c} - D_0 Tim^i_c, \tag{A.4}$$

$$\frac{dPT^i_c}{dt} = V_1 Per^i_c Tim^i_c - V_2 PT^i_c - T_1 \frac{PT^i_c}{K_1 + PT^i_c} + T_2 \frac{PT^i_n}{K_2 + PT^i_n} - D_5 \frac{PT^i_c}{L_5 + PT^i_c} - D_0 PT^i_c, \tag{A.5}$$

$$\frac{dPT^i_n}{dt} = T_1 \frac{PT^i_c}{K_1 + PT^i_c} - T_2 \frac{PT^i_n}{K_2 + PT^i_n} - D_6 \frac{PT^i_n}{L_6 + PT^i_n} - D_0 PT^i_n, \tag{A.6}$$

$$\frac{dClk^i_m}{dt} = S_5 \frac{(PT^i_n/A_3)^a + B_3}{1 + (CC^i_n/R_3)^r + (PT^i_n/A_3)^a + B_3} - D_7 \frac{Clk^i_m}{L_7 + Clk^i_m} - D_0 Clk^i_m, \tag{A.7}$$

$$\frac{dClk^i_c}{dt} = S_6 Clk^i_m - V_3 Clk^i_c Cyc_c + V_4 CC^i_c - D_8 \frac{Clk^i_c}{L_8 + Clk^i_c} - D_0 Clk^i_c, \tag{A.8}$$

$$\frac{dCC_c^i}{dt} = V_3 Clk_c^i Cyc - V_4 CC_c^i - T_3 \frac{CC_c^i}{K_3 + CC_c^i} + T_4 \frac{CC_n^i}{K_4 + CC_n^i} - D_9 \frac{CC_c^i}{L_9 + CC_c^i} - D_0 CC_c^i. \quad \text{(A.9)}$$

To describe transcription, we used Hill-type equations that are characterized by six parameters representing the maximum velocity ($S_l, l = 1, 3, 5$), two DNA binding constants for an activator and a repressor (A_l and $R_l, l = 1 \ldots 3$), two Hill coefficients for activation and repression (a and r) and one constant ($B_l, l = 1 \ldots 3$), which indicates transcriptional activation by transcription factors other than PER–TIM or dCLK–CYC. The translation rate ($S_l, l = 2, 4, 6$) was assumed to be proportional to mRNA concentration. Association and dissociation rates ($V_l, l = 1 \ldots 4$) were made to obey the law of mass action. Degradation and nuclear transportation were supposed to be mediated by degradation enzymes and transporters, respectively. We described these processes with Michaelis–Menten-type equations characterized by the maximum velocity (for degradation, $D_l, l = 1 \ldots 10$, and for transportation, $T_l, l = 1 \ldots 4$) and the binding constant (for degradation, $L_l, l = 1 \ldots 10$, and for transportation, $K_l, l = 1 \ldots 4$). Non-specific degradation terms are proportional to each variable with proportionality constant D_0. We used 100 cellular models for multicellular models ($i = 1 \ldots 100$ in eqns (A.1)–(A.9)). Values of all of the 48 system parameters are chosen to reproduce *per*, *tim*, and *dClk* mRNA time courses in wild-type and steady-state levels of these mRNAs in mutants in the absence of internal noise (Ueda *et al.*, 2001). Parameter values are: $Cyc_c = 1\,nM$, $S_1 = S_3 = 1.45\,\mathrm{nM\,hr^{-1}}$, $S_2 = S_4 = 0.48\,\mathrm{hr^{-1}}$, $S_5 = 1.63\,\mathrm{nM\,hr^{-1}}$, $S_6 = 0.47\,hr^{-1}$, $r = 4$, $R_1 = R_2 = 1.02\,\mathrm{nM}$, $R_3 = 0.89$ nM, $a = 1$, $A_1 = A_2 = 0.45\,\mathrm{nM}$, $A_3 = 0.8\,\mathrm{nM}$, $B_1 = B_2 = 0$, $B_3 = 0.6$, $V_1 = 1.45\,\mathrm{nM^{-1}\,hr^{-1}}$, $V_2 = 1.45\,\mathrm{hr^{-1}}$, $V_3 = 1.63\,\mathrm{nM^{-1}\,hr^{-1}}$, $V_4 = 1.63\,\mathrm{hr^{-1}}$, $T_1 = 1.73\,\mathrm{nM\,hr^{-1}}$, $T_2 = 0.72\,\mathrm{nM\,hr^{-1}}$, $T_3 = 1.63\,\mathrm{nM\,hr^{-1}}$, $T_4 = 0.52\,\mathrm{nM\,hr^{-1}}$, $K_1 = 2\,\mathrm{nM}$, $K_2 = 2\,\mathrm{nM}$, $K_3 = 2\,\mathrm{nM}$, $K_4 = 2\,\mathrm{nM}$, $D_1 = D_3 = 0.94\,\mathrm{nM\,hr^{-1}}$, $D_2 = D_4 = 0.44\,\mathrm{nM\,hr^{-1}}$, $D_5 = 0.44\,\mathrm{nM\,hr^{-1}}$, $D_6 = 0.29\,\mathrm{nM\,hr^{-1}}$, $D_7 = 0.54\,\mathrm{nM\,hr^{-1}}$, $D_8 = 0.6\,\mathrm{nM\,hr^{-1}}$, $D_9 = 0.6\,\mathrm{nM\,hr^{-1}}$, $D_{10} = 0.3\,\mathrm{nM\,hr^{-1}}$, $L_1 = L_3 = 0.3\,\mathrm{nM}$, $L_2 = L_4 = 0.2$ nM, $L_5 = 0.2\,\mathrm{nM}$, $L_6 = 0.2\,\mathrm{nM}$, $L_7 = 0.13\,\mathrm{nM}$, $L_8 = 0.2\,\mathrm{nM}$, $L_9 = 0.2\,\mathrm{nM}$, $L_{10} = 0.2\,\mathrm{nM}$ and $D_0 = 0.012\,\mathrm{hr^{-1}}$.

To introduce internal noise, the rates of all reactions, $S_l (l = 1 \ldots 6)$, $T_l (l = 1 \ldots 4)$, $V_l \times (l = 1 \ldots 4)$ and $D_l (l = 0 \ldots 10)$, were varied at each time step of simulation (0.1 hr) in such a way that their values are normally distributed around their mean with a 10% standard deviation. For example, S_1 is normally distributed around its mean (= 1.45) with a standard deviation (= 0.145). We used an Euler scheme to integrate these stochastic differential equations with multiplicative noise. We used 0.1 hr as the time interval. Multiplicative noise associated with rates of reactions is used for simulating the randomness inherent in biochemical reactions involving a small number of molecules.

An alternative way to treat internal noise is Gillespie's (1977) method, where the internal noise of reaction is naturally calculated from the number of molecules participating in that reaction. However, Gillespie's method requires full knowledge of detailed molecular mechanisms that are not available so far and much more computational power to simulate. Compared with Gillespie's method, the main disadvantage of our method is the incapability to determine the magnitude of internal noise from first principles.

To compensate for this shortcoming, we can assess the magnitude of internal noise by using previously reported experimental data. Although no information is available regarding the magnitude of internal noise in *Drosophila*, we assessed the magnitude of noise based on the following consideration. Our simulation system with 10 or 30% noise exhibits *per* mRNA oscillations with a period of 24.0 $\pm$ 0.5 or 24.0 $\pm$ 1.5 hr (mean $\pm$ S.D., determined by a chi-square periodogram using 100-cell time series data over 5 days). These variations are similar to what was observed in the neural activity of single mammalian neurons in culture (24.35 $\pm$ 1.20 hr, mean $\pm$ S.D.) (Welsh *et al.*, 1995). Preliminary

results suggest that the basic conclusions (a synchronizing factor is secreted from individual cells during subjective day to induce light-pulse-type phase shifts in the neighboring cells, or, alternatively, a factor is secreted during subjective night to induce dark-pulse-type phase shifts) obtained from the system with 10% noise also hold for the system with 30% noise. In the presence of 30% noise and in the absence of synchronization, the averaged *per* mRNA oscillation is reduced to less than 5% within several days, which is within the physiological range for damped circadian oscillators.

Appendix B

Search for Synchronizing Factors

To synchronize circadian oscillators, we introduced a factor (X^i) into the system described above (eqns (A.1)–(A.9)). The kinetics of the synchronizing factor is described as follows.

$$\frac{dX^i}{dt} = S_X \frac{(Y^i/A_X)^{a_X}}{1+(Y^i/A_X)^{a_X}} - D_X \frac{X^i}{L_X + X^i} - D_0 X^i + D_c \sum_j (X^j - X^i). \quad \text{(B.1)}$$

Secretion of the factor was supposed to be activated or repressed by one of the 10 variables described above ($Y^i \in \{Per_m^i, Tim_m^i, Clk_m^i, Per_c^i, Tim_c^i, Clk_c^i, PT_c^i, PT_n^i, CC_c^i, CC_n^i\}$). To describe the kinetics of secretion (the first term on r.h.s of eqn (B.1)), we used Hill-type equations that were characterized by three parameters: the maximum velocity (S_X) and the DNA binding affinity of activators or repressors (A_X), and the non-linearity of activation or repression ($|a_X|$). If Y^i activates the secretion of the factor, a_X is positive ($a_X = |a_X|$). On the other hand, if Y^i represses the secretion, a_X is negative ($a_X = -|a_X|$). In this case, the first term of eqn (B.1) can be transformed to

$$S_X \frac{1}{1+(Y^i/A_X)^{|a_X|}}.$$

Degradation of the factor was supposed to be mediated by degradation enzymes with the maximum velocity (D_X) and the Michaelis constant (L_X). The non-specific degradation term is proportional to X^i with the proportionality constant D_0. Synchronizing factors were supposed to spread through diffusion in three-dimensional space with the diffusion constant (D_c), and 100 cells were placed in a hexagonal lattice [index j in eqn (B.1) indicates neighboring cells]. Namely, we performed reaction–diffusion simulations on a hexagonal lattice, each point of which represents a cell. We used a straightforward discretization of the Laplacian operator and each point (cell) in the hexagonal lattice is surrounded by 12 points (cells) on average. Some parameter values were: $|a_X| = 4$, $D_X = 0.6\,\text{nM}$ hr^{-1}, $L_X = 0.5\,\text{nM}$, $D_c = 0.5\,\text{hr}^{-1}$. Values of two parameters (S_X and A_X) were dependent on an activator or a repressor of the factor. These values are chosen so that the peak concentration of the factor is 4.0 nM and the half-maximal duration is 8.0 hr (see Table B1).

The factor was supposed to increase or decrease the rate of one of the reactions in

TABLE B1

Activator	S_X (nM hr^{-1})	A_X (nM)	Repressor	S_X (nM hr^{-1})	A_X (nM)
Per_m^i	1.5358	3.4553	Per_m^i	0.9417	0.6448
Per_c^i	3.9962	2.4813	Per_c^i	1.1093	0.4815
Tim_m^i	1.5358	3.4553	Tim_m^i	0.9417	0.6448
Tim_c^i	3.9962	2.4813	Tim_c^i	1.1093	0.4815
PT_c^i	1.1245	1.7272	PT_c^i	0.9646	0.2306
PT_n^i	1.7796	2.8529	PT_n^i	1.0179	0.4757
Clk_m^i	3.9962	6.7186	Clk_m^i	0.9265	1.0778
Clk_c^i	3.9962	4.2784	Clk_c^i	0.9646	0.4906
CC_c^i	2.8765	2.8857	CC_c^i	0.9646	0.2822
CC_n^i	3.9962	4.4730	CC_n^i	1.0636	0.8192

the circadian system. Parameters regulated by the factor include $S_l(l = 1 \ldots 6)$, $T_l(l = 1 \ldots 4)$, $V_l(l = 1 \ldots 4)$, $D_l(l = 0 \ldots 10)$, $A_l(l = 1 \ldots 3)$, $R_l \times (l = 1 \ldots 3)$, $B_l(l = 1 \ldots 3)$, $K_l(l = 1 \ldots 4)$ and $L_l \times (l = 1 \ldots 10)$.

For activation, we substituted the target parameter P (e.g. S_1) with the following logistic-type function:

$$\left(1 + \frac{M - 1}{1 + \exp[-k(X^i - X_h)]}\right)P$$

$$= \frac{M + \exp[-k(X^i - X_h)]}{1 + \exp[-k(X^i - X_h)]}P. \quad (2a)$$

This function was characterized by three parameters: maximum velocity M, threshold concentration X_h and nonlinearity for increase k.

For repression, we substituted the target parameter P with the following function:

$$\frac{1 + \exp[-k(X^i - X_h)]}{M + \exp[-k(X^i - X_h)]}P. \quad (2b)$$

This function was characterized by three parameters: minimal velocity $1/M$, threshold concentration X_h and nonlinearity for decrease k. Parameter values were: $M = 2$, $X_h = 2\,\text{nM}$ and $k = 3$.

Appendix C

Calculation of Phase Shifts

Phase shifts were calculated by increasing (or decreasing) the target reaction rate by 2-, 4-, 6-, 8-, or 10-fold for 1 hr from 100 different circadian time points and measuring the peak time of *per* mRNA oscillation, which was compared with the peak time of *per* mRNA oscillation without perturbation. Phase shifts became larger as the intensity of the factor became greater, but the shapes of the phase shift–circadian time relationship remained similar. Ninety-six patterns of phase shifts were obtained by increasing or decreasing all of the 48 system parameters that represent the rates of reactions constituting the circadian clock. In Fig. 3, phase shifts obtained by increasing (or decreasing) the reaction rate targeted by synchronizing factors are depicted. Periods of *per* mRNA oscillations are determined from the chi-square periodogram.